

INVESTIGATION OF STRUCTURAL PERFORMANCE OF HISTORICAL AMASYA HUNDI HATUN BRIDGE

Burçin Şenol ŞEKER^a, Merve ÖZKAYNAK^{a*}

^a Associate Prof.; Faculty of Architecture, Amasya University, Amasya, Turkey

*Corresponding author. E-mail address: merve.ozkaynak@hotmail.com

Received: 27.05.2021; Revised: 23.11.2021; Accepted: 4.02.2022

Abstract

Bridges have been built by many civilizations throughout history to connect the two banks of a river. There have been numerous historical bridges built in Anatolian geography because the area has served as a bridge to various civilizations. This study performed a structural evaluation of the Hundi Hatun Bridge in Amasya, Turkey. First, a 3D model of the bridge was created in a digital environment, and then static and dynamic analyses were performed with software using the ANSYS Workbench finite element method. The bridge demonstrated sufficient dimensions under static loads and in the modal analysis, although the arches were subject to translational movement in the flow direction of the river. In addition, linear and nonlinear material models were used to perform dynamic analyses, including bridge seismic analyses. The linear material model indicated that the bridge is safe, while the nonlinear material model revealed that damage may occur, especially at the abutments and peak regions of the bridge. Moreover, the bridge arch flatness was determined to be a very important parameter. The results of this study can be used to guide future restoration efforts.

Keywords: Cultural Heritage; Historical Bridge; Static and Dynamic Analysis; Linear and Nonlinear Material; Restoration.

1. INTRODUCTION

There are many historical stone bridges from the Roman, Byzantine, Seljuk, and Ottoman periods in Anatolian geography, partially because the area has served as a transition route between the Asian and European continents. Many of these structures have survived until today because of restorations and improvements. The most important characteristic of these structures was their role in facilitating trade and military transportation. In addition, they can be considered water structures, because they were built on rivers and thus exposed to hydraulic loads. These historical stone bridges were generally constructed according to three main architectural types: i) the type with continuous arches that have arch spans and peak regions in the sequence at the same or nearly the same level, ii) the type with an odd number of bays that rise towards the top elevation of the bridge and have the largest arch bay in the middle, iii) the type with an

even number of bays that rise towards the top elevation of the bridge and have the largest arch bay in the middle. The bridge analyzed in this paper is an example of the third type [5].

There are primarily two different types of research on historical bridges. In the first group of studies, the structural behaviors of bridges are modeled in a finite element environment by performing a detailed analysis of the bridges' building materials. Then the bridges' deformation patterns and crack and stress distributions are determined by performing static and dynamic analyses on the models [2, 10, 14, 17, 23, 24, 25]. In the second group of studies, deteriorations and deformations on historical bridges are determined through observations, and the improvement and restoration work required to eliminate these defects are examined in detail [1, 16, 20, 21, 26, 40]. In one study, Altunisik, Kanbur, and Genc [6] examined the effects of varying thicknesses of arches (one of the main load-bearing

elements of a historical bridge) on the structural behavior of the bridge. In another study, Oliveira, Lourenço, and Lemos [22] examined 59 different historical bridges. After reviewing the bridges' historical design formulas, they determined the load-carrying capacities of 8 reference bridges. The results of their research indicated that bridge arch thickness and the physical properties of fill material are important parameters. A different study collected detailed information on a historical bridge by using photometric, laser scanning, and radar scanning examination techniques, which allowed the researchers to observe the damage occurring over time and make appropriate restoration interventions [27]. The authors of another study investigated the possibility of increasing the axle load of a historical railway bridge from 200 to 250 kN. To determine this possibility with accuracy, the necessary measurements were made on the bridge to calibrate a 3D model created in a computer environment. The results indicated that this load increase was possible [8]. In the present study, a 3D model of the historical Hundi Hatun Bridge was created in a finite element environment and then subjected to static and dynamic analyses to determine the potential damage areas of the structure. Moreover, the analyses determined the plastic joint points that could occur on the bridge under different traffic loads.

2. LOAD-BEARING SYSTEM DETAILS OF A HISTORICAL BRIDGE

Figure 1 shows the construction details of a typical historical bridge. As can be seen from the figure, bridge elements consist of a main load-carrying arch, spandrel, and wing walls. To provide arch stability and increase strength, non-cohesive fill material was used in the inner region. On the bridges, cutwaters are used to reduce the impact of upstream water, and parapet elements are used for pedestrian safety.

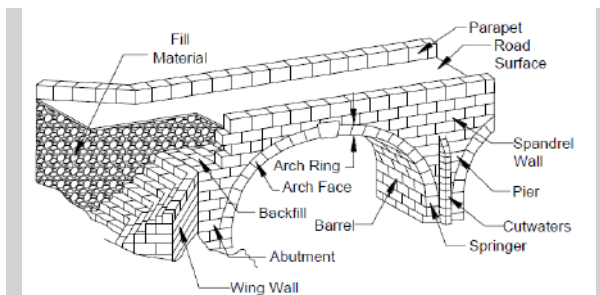


Figure 1. Construction details of a typical historical bridge [19]

3. HISTORICAL AND ARCHITECTURAL PROPERTIES OF THE HUNDI HATUN BRIDGE

The Yeşilırmak river flows in the southwest-northeast direction and divides the city of Amasya (Fig. 2) into two regions. Therefore, bridges have been built in various places on the river to connect these two separate regions. One of these bridges, the Hundi Hatun Bridge, is located on the Yeşilırmak River in the eastern region of the city. The Bayezid Pasha Mosque is located in the south and the Büyük Ağa Madrasah in the north. The Hundi Hatun Bridge was built by Sultan Mesut's daughter, Hundi Hatun. It was repaired in 1900 and 1959. It has four bays and flat, circular arches. It is 67 m long, 8 m wide, and 10.50 m high [12]. The general view of the bridge is shown in Fig. 3.



Figure 2. Map of Turkey and location of Amasya city [35]

4. THE HUNDI HATUN (KUNÇ) BRIDGE – FINITE ELEMENT MODEL AND MATERIAL PROPERTIES

4.1. Finite Element Model

Historical artifacts are structures built with a combination of different materials. Some parts of the structures can be made of stone, while other parts can be built with brick. Mortar is usually used as the binding material. Detailed micro modeling, simplified micro modeling, and macro modeling techniques are used to model all these different material types in a finite element environment. These techniques are shown in Figure 4.

In detailed micro modeling, the mechanical properties of masonry elements and mortar are discussed separately. This technique is widely used to determine the behavior of masonry walls. Because of the

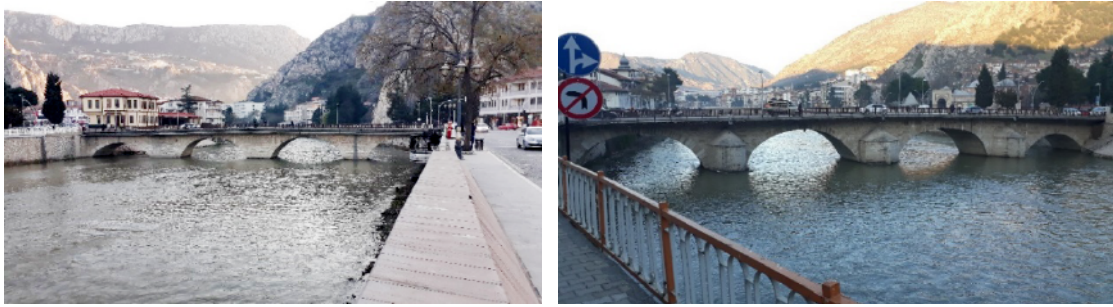


Figure 3.
Hundi Hatun Bridge – Downstream and upstream views [32]

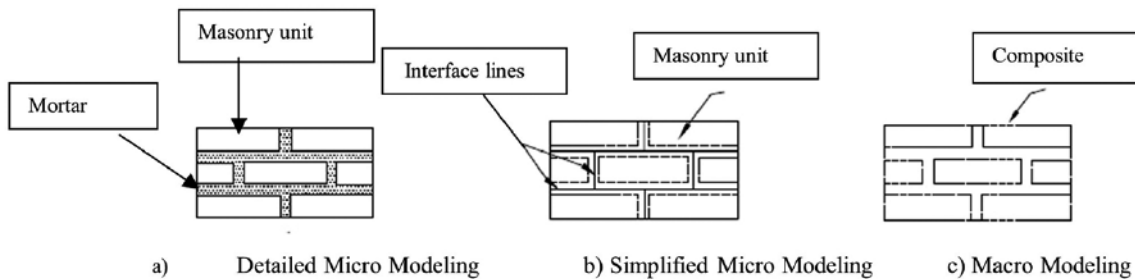


Figure 4.
Masonry structure modeling technique

long analysis times required for micro modeling, it is appropriate to use this method to analyze small-scale structures or for small regions of large-volume structures where detailed information is required.

In the simplified micro modeling technique, new masonry elements are obtained by adding a half thickness of the mortar layer to the masonry elements. The masonry units are separated from each other by interface lines. It is accepted that the cracks in the structure will occur at these interfaces.

In the macro modeling technique, masonry unit elements and mortar are composite materials, and new mechanical properties are assigned to this new element depending on the strength of the units. This technique is the preferred method for large-scale structures because it decreases the amount of analysis time required in the digital environment [29]. In this study, analyses were carried out using the macro modeling technique.

4.2. Material Properties

The Hundi Hatun Bridge's main material is sandstone, which was used for the arches and wing walls. The inner region contains filling material. Since this is a historical structure there is no permission for these types of historical structures to examine in detail with destructive experimental methods from

the government. So, to get an information about the reaction of the structure to external loads, the material characteristics given in the literature is used. These values are obtained from the restoration works of similar historical structures constructed in the same region in the same dates. So, these values can be used. The test results for the material used in another historical bridge in the same city were used to determine the mechanical properties of the material used in the Hundi Hatun Bridge. According to these test results, the average compressive strength for the stone was 41.46 MPa, while its density was 2646 kg/m³ [2]. For the fill material, the elasticity modulus (E) was 800 MPa, Poisson's ratio was 0.23, and the density was 1800 kg/m³ [29].

In one study [23], the equation given to determine a wall's characteristic compressive strength is:

$$f_k = 0.5 \times f_b^{0.65} \times f_m^{0.25} \quad (1)$$

Accordingly, E is calculated as:

$$E = 1000 \times f_k \quad (2)$$

where f_b is the compressive strength of the stone, and f_m is the compressive strength of the mortar. The tensile strength of the wall was accepted as 10% of its compressive strength. The bridge's material properties are shown in Table 1. For the mortar, the compressive strength was used 6 MPa [33].

Table 1.
Physical and mechanical properties of homogenized materials used in the bridge

Bridge Region	Elasticity Modulus (MPa)	Poisson's Ratio	Density (kg/m ³)	Mean Compressive Strength (MPa)	Mean Tensile Strength (MPa)
Arches and Wing Walls	8810	0.15	2646	8.810	0.881
Fill	800	0.23	1800	0.8	0.08

5. STRUCTURAL ANALYSES

5.1. Linear Static Analyses

Software generating solutions using the finite element method are widely implemented today to examine historical buildings with quite complex geometric and material properties. The general behaviors and

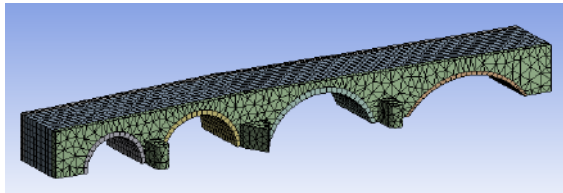


Figure 5.
Finite element model of the Hundi Hatun Bridge

critical regions of historical buildings under static and dynamic loads can be determined. The three-dimensional bridge model created in this study was subjected to linear and non-linear analyses in an ANSYS environment [7]. For the linear analysis, a Solid 186 element type with three degrees of freedom at each node was used. The finite element model of the historical Hundi Hatun Bridge is shown in Figure 5.

An analysis of the bridge under its weight was used to determine the principal stress, total deformation, and shear stress distributions of the bridge. The maximum values in the principal stress distribution (shown in Figure 6) occur on the road surface at the peak points of the regions between the bridge arches. Considering that the tensile strength for stone and filling material is very low, cracks should be expected in these regions. However, in ancient artifact building techniques, this problem was eliminated by connecting stone elements with iron clamps. The maximum principal stress value was found to be 1.2909 MPa.

5.2. Modal Analysis

In modal analysis, the free vibration periods and mode shapes of the structure are determined by using elastic material properties. Thus, preliminary information about the dynamic behavior of the structure can be obtained. Figure 8 shows the structure's modal

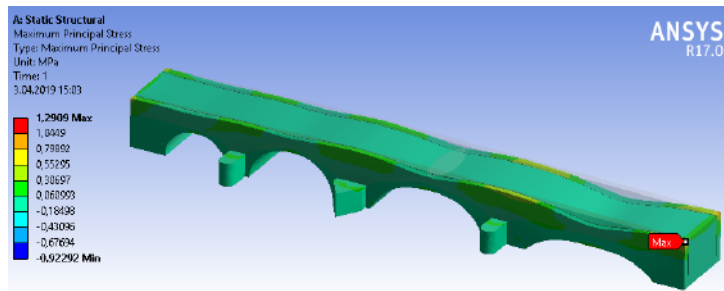


Figure 6.
Maximum principal stress distribution

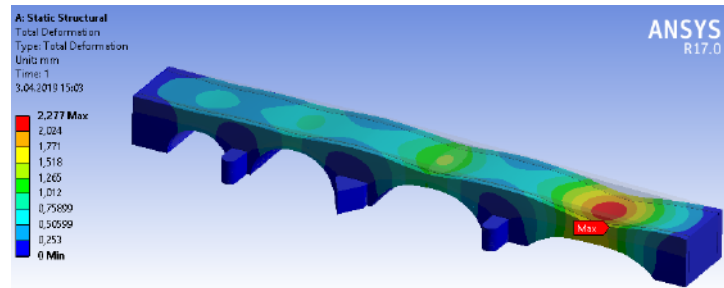


Figure 7.
Modal Analysis

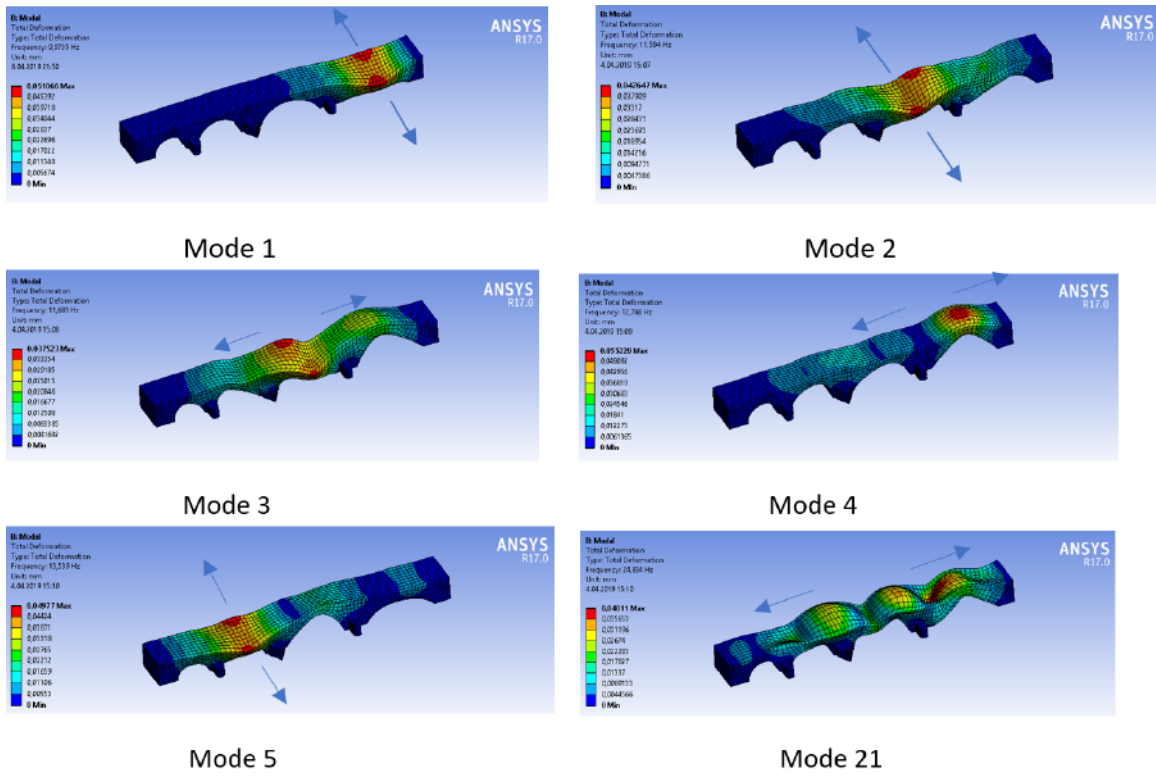


Figure 8. Mode shapes

shapes with the highest mass participation ratios, while their periods and mass participation ratios are shown in Table 2. As given in Table 2, first and second mode shapes are in the X direction that is transversal direction. The third longitudinal mode shape is in the Y direction. All of the mode shapes' directions are in the orthogonal plane.

Figure 8 shows that the first, second and fifth modes, which were effective in the X-direction of the bridge, occurred in the arch regions. The maximum deformation values were high up in the upper points of the arches because the arch springer points were fixed support. High stress and deformation values are expected in these regions under the effects of an earthquake.

Table2. Hundi Hatun Bridge – mass participation ratios

Mode	Period (s)	Mass Participation Ratios	
		X - direction	Y - direction
1	0.10027	0.254380	~0.00
2	0.086250	0.109023	0.160643
3	0.085595	~0.00	0.228147

5.3. Seismic Assessment of the Bridge

Earthquakes are natural and unpredicted disasters. Because earthquakes are a vibration of the earth's crust, they damage structures by creating a time-dependent deformation movement. The formation of earthquakes is explained by plate tectonics. The crust on the mantle layer in the center of the earth is made up of many mobile plates. During the movements of these plates, energy accumulates at the edges and inside the plates, and when the strength of the crust is overcome, energy is released, and earthquakes occur.

Turkey has experienced severely destructive earthquakes because of its geography and tectonic structure. There are African and Arabian plates in southern Turkey. Both plates move northwards and compress the Anatolian block. The compression rate of the Arabian plate is high, while the rate of the European-Asian Plate in the north, also called the Eurasian Plate, is very low. As a result of this phenomenon, the Anatolian Block has to move westwards; accordingly, the North Anatolian Fault Zone and the East Anatolian Fault Zone are formed (see Figure 9). Highly destructive earthquakes occur on these fault lines [11]. Therefore, it is important to

examine the seismic behavior of the structures in Turkey, which is in such a fragile geographic region, by considering both the structure's historical heritage and its subjection to strong dynamic effects, like earthquakes.

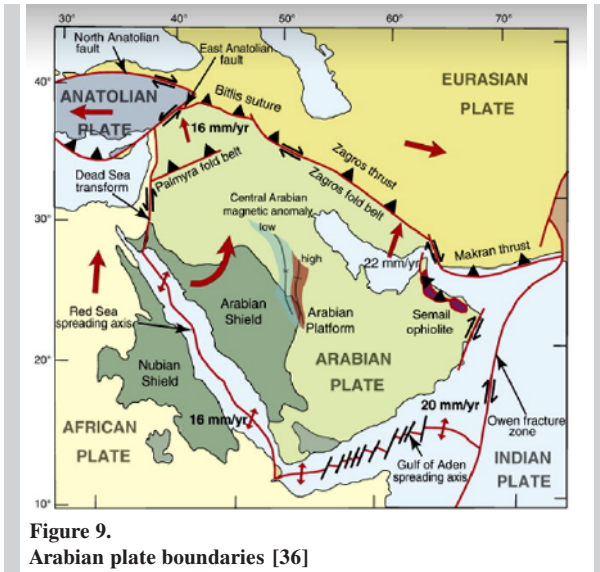


Figure 9. Arabian plate boundaries [36]

Turkey has been divided into five distinct regions in terms of earthquake hazard by considering fault lines and previous earthquakes. The first-degree seismic zone indicates the most dangerous zone, while the fifth-degree seismic zone indicates the zone with the lowest hazard. The most hazardous areas are shown in red (see Fig. 10). The map of Turkey in Fig. 10 reveals that only a small area in the middle region has a very low earthquake hazard, while all of the other regions have a high risk of earthquakes. The first-degree seismic zone includes the North Anatolian

Fault (which starts at Lake Van and extends to the Marmara Sea and the Dardanelles) and the active faults affecting the Aegean Region. The most active fault in Turkey is the North Anatolian Fault, which is located in the northern region of Turkey and is 1,500 kilometers long. The number of earthquakes on this fault line increased after the great Erzincan earthquake in 1939. Historically, earthquakes of 7 or higher magnitude occur in Turkey approximately every three or four years. Since 1900, nearly 100,000 people in Turkey have died in an earthquake, which demonstrates the fragility of the region to earthquakes [11].

In the linear and nonlinear analyses described in this section, the 1992 Erzincan seismogram was used. The seismogram of the earthquake accelerated in the north-south direction, which is in the same direction as the Hundi Hatun Bridge. The maximum acceleration in this direction was 0.47 g. The time step was 0.005 and the damping ratio was 0.05. A full Newton-Raphson method was used in the analyses as the solution algorithm. The analysis results were used to calculate the stresses and deformations in the structure. Earthquake acceleration values are shown in Fig. 11.

Linear and nonlinear seismic analyses of the historical Hundi Hatun Bridge were performed with the ANSYS Workbench software. The Drucker-Prager and Mohr-Coulomb nonlinear material models have been used in the analyses of masonry structures in many studies [4, 9, 30]. In this study, the Mohr-Coulomb model was used for the material properties of the stone and fill material.

The Mohr-Coulomb failure criterion (see Fig. 12) is based on the principle that failure occurs because of the shear in a plane where the boundary shear stress

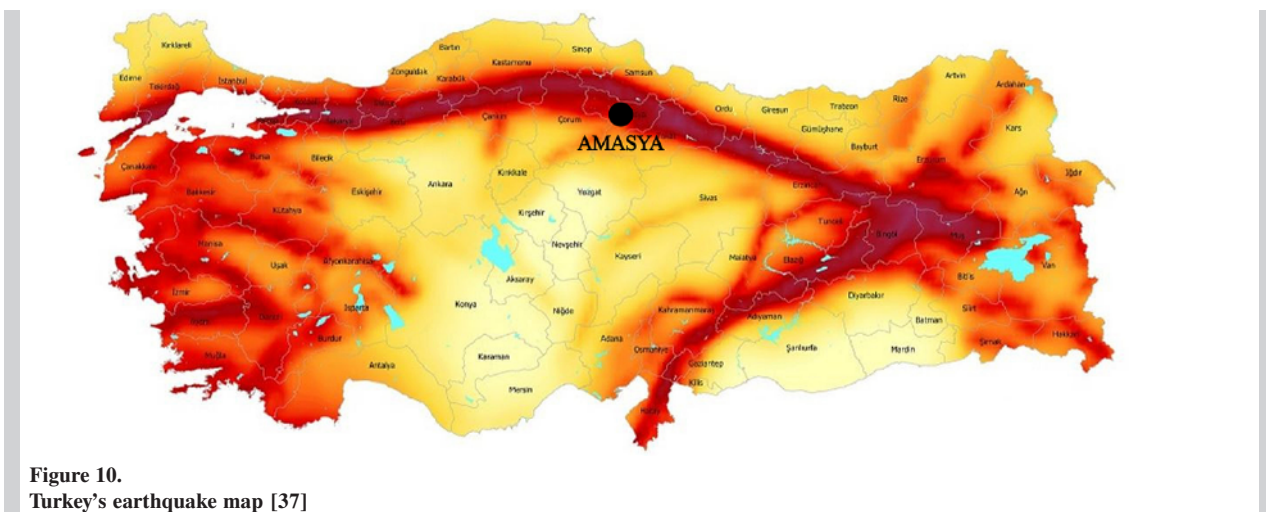


Figure 10. Turkey's earthquake map [37]

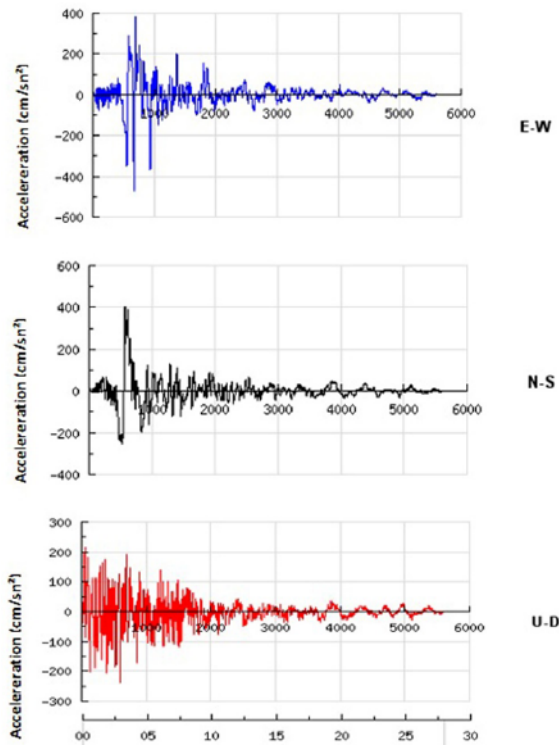


Figure 11.
The acceleration values of the 1992 Erzincan earthquake (cm/s²) [37]

is exceeded. The boundary shear stress is the sum of intergranular adhesive strength, (cohesion, c) and frictional resistance increases with the level of axial stress (σ) acting on the shear plane. The boundary shear stress at which failure occurs is calculated by Equation 1. The term ϕ is the internal friction angle specific to the material.

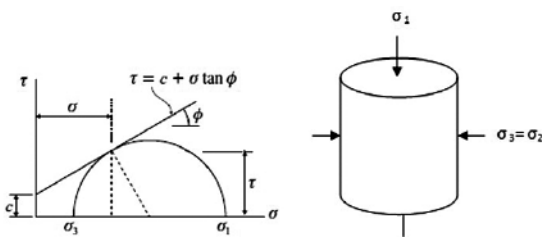


Figure 12.
The Mohr-Coulomb failure criterion [13]

$$f(\sigma) = \tau = c + \sigma \tan \phi \quad (1)$$

The Mohr-Coulomb failure criterion is a two-parameter model. When the parameters c and ϕ are known, the failure surface can be defined. The given envelope equation can also be written in terms of

principal stresses. The Mohr-Coulomb failure criterion is defined independently from the median principal stress. With the appropriate mathematical transformations, the Mohr-Coulomb failure criterion can be determined in a triaxial principal stress environment (see Figure 13) [13]. To give the nonlinearity to a brittle masonry material in the finite element environment, we use the Mohr Coulomb or Drucker Prager material model. There are a lot of studies that has been accepted in the literature. So, with the consistent values of ϕ and c , this material model can be used to investigate the behaviour of these historical structures. This model is quite good and suitable for this type of study as can be seen in the literature [3, 10, 15, 18, 19, 28, 31]. The c and ϕ parameters used for the stone and fill regions in this study are shown in Table 2.

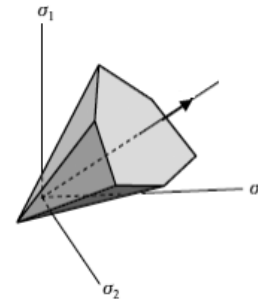


Figure 13.
The Mohr-Coulomb failure hypothesis collapse plane [13]

Table 3.
The Mohr-Coulomb material model properties for the homogenized materials used in the Hundi Hatun Bridge [15, 28]

Bridge	Cohesion (C) (MPa)	Friction Angle (ϕ)
Arches and Wing Walls	0.15	30
Fill	0.05	20

5.3.1. Linear Time History Analysis

The maximum deformation values obtained from the linear time history analysis are shown in Fig. 14. The highest deformation occurs at the peak of the arch on the far right, which has the highest flatness. The maximum deformation value in the linear time history analysis was 2.13 mm in transversal direction. The maximum tensile principal stresses are shown in Figure 15. The maximum values are observed at the support points of the arch on the far left on the downstream side. The maximum tensile principal stress value was 2.82 MPa. The maximum equivalent (von

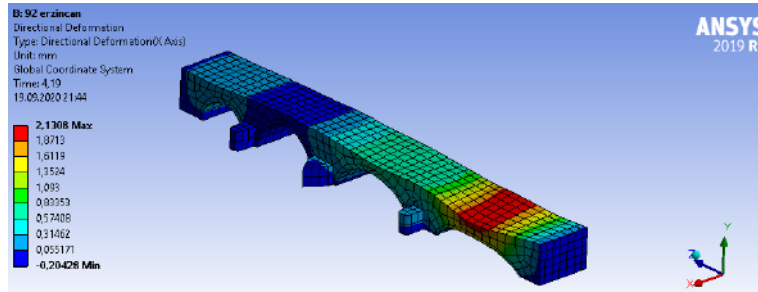


Figure 14.
X-Direction maximum deformation distribution

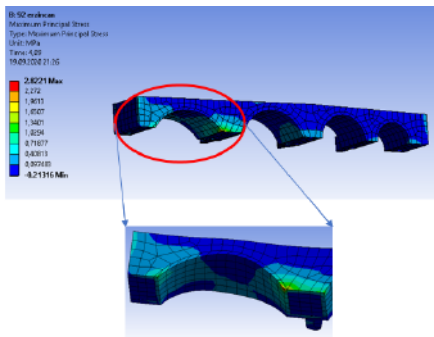


Figure 15.
1st principal stress distribution

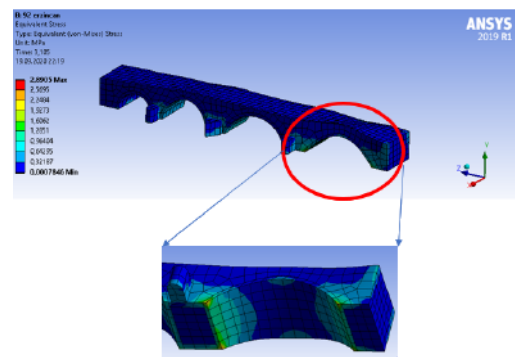


Figure 16.
Equivalent stress distribution

Mises) stresses are shown in Fig. 16. The maximum equivalent stresses occur at the support points of the abutments on which the middle arch sits. The maximum equivalent stress value was 2.89 MPa.

5.3.2. Nonlinear Time History Analysis

The deformation value distribution obtained from the nonlinear time history analysis is shown in Fig. 17. The maximum deformation values occur at the peak of the main arch in the middle. The absolute maximum deformation value was 8.19 mm in transversal direction. Fig. 18 shows the maximum plastic strain propagation. The maximum plastic strains

were observed at the support points of the abutments on which the middle arch sits.

When examining the principal stress and equivalent stress (von Mises) distributions in Figs. 19 and 20, the maximum stress values occur around the abutments and decreasingly move towards the upper points of the bridge.

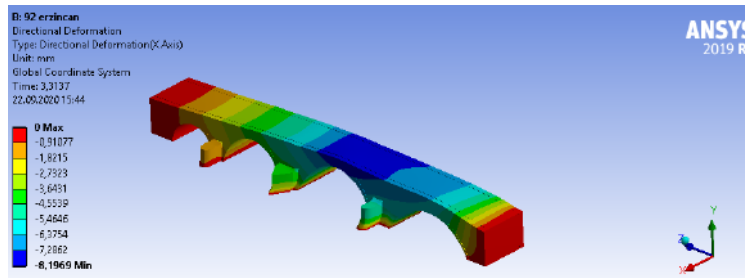


Figure 17.
Maximum x-direction deformation distribution

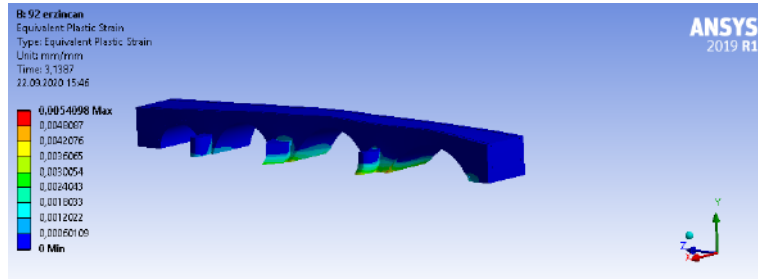


Figure 18. Maximum plastic strain propagation

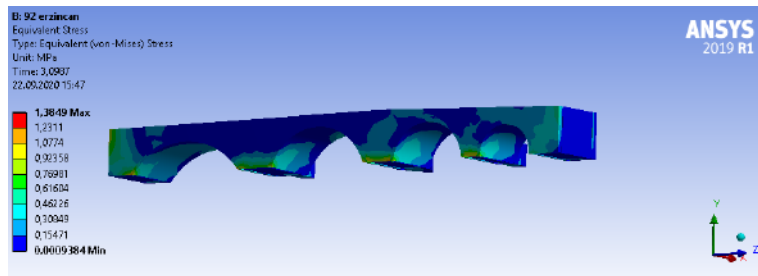


Figure 19. Equivalent stress distribution

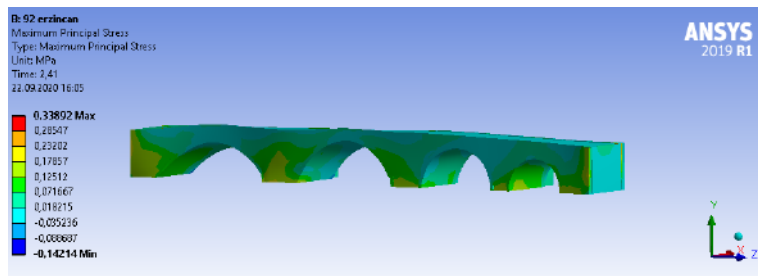


Figure 20. 1st principal stress distribution

6. DISCUSSION

In this study, the Hundi Hatun Bridge was analyzed by creating a 3D model in a computer environment and assigning linear and nonlinear material properties to the masonry units constituting the bridge. The macro modeling technique was used, and the units constituting the structure were considered. By analyzing historical structures, their load-carrying system capabilities can be determined according to their strength and strain values. In the strength evaluation, the maximum stresses formed should not exceed the allowable stress value of the deformation evaluation; the ratio of the maximum deformation to the maximum height of the bridge should not exceed a certain value [38]. The Earthquake Risk Management Guide for Historic Structures defines the limits for the maximum deformation ratio allowable for varying perfor-

mance levels in the context of dynamic effects (see Tab. 4).

Table 4. Historical structures performance levels and deformation limits

Performance Level	Maximum Deformation / Maximum Height Ratio Limit
Limited Damage	0.003
Controlled Damage	0.007

The performance levels given in Tab. 4 are defined as follows:

1. Limited Damage: In this damage level, limited nonlinear behavior (damage) occurs in the load-carrying system elements of the structures.

2. **Controlled Damage:** In this damage level, the damage only occurs in repairable load-carrying system elements of the structures.
3. **Prevention of Collapse:** In this damage level, severe damage occurs in the load-carrying system elements of the structure, and the structure is about to collapse partially or completely, but the collapse is prevented.

The deformation ratio in historical structures is the ratio of the difference in horizontal deformations at different levels to the height difference. Because the foundation of the structures is fixed at the ground, the deformations in this plane are zero. Therefore, the height and deformation differences between the top and bottom points of the bridge are considered in the study.

The bridge height in this study is 10 m. Therefore, the maximum deformation limits according to Tab. 4 are 3 mm for limited damage, 7 mm for controlled damage, and 10 mm for prevention of collapse.

The following results are interpreted according to the above principles:

- In the case of linear static loading, maximum compressive and tensile stresses formed at the far-right arch springer points on the upstream side, depending on the bridge arch geometry. Similarly, maximum deformations occurred at the peaks of the far-right arch. The bridge was safe under linear static loads, as it did not exceed allowable values.
- Modal deformations occurred in the load-carrying arches perpendicular to the flow direction of the river. The bridge was strained, so it experienced out-of-plane deformation in the direction of its weakest axis. It was determined that these deformations may distort the arch geometry in both orthogonal directions. Therefore, the modal analysis shows that the stones constituting the arch elements should be interlocked.
- The linear time history analysis demonstrated that the tensile stresses formed at the support points of the right end arch on the upstream side and exceeded the allowable stress value.
- The linear time history analysis also showed that the highest deformation values occurred in the arch with the highest flatness. The highest deformation value obtained in this study was below 3 mm, placing it within the limited damage level.
- The nonlinear analysis revealed that the maximum principal and equivalent stresses had high values at all bridge abutments and exceeded the allowable stress values. Plastic deformations occurred at the

support points of the far-right arch according to the perspective of the middle arch and upstream side. The nonlinear analysis also indicated that the largest deformations occurred at the peaks of these arches. The displacement value of 8 mm was considerably higher than that obtained by linear analysis, so the bridge exceeded the upper limit value for controlled damage.

7. CONCLUSION

In Turkey, bridges of historical importance are currently open to traffic. It is important to examine these structures because they are mostly found in cities and thus must necessarily be used, even under far greater traffic loads than what was expected when they were built. This study evaluates the structural performance of the historical Hundi Hatun Bridge, located in the city center of Amasya. The Hundi Hatun Bridge connects the two separate sides of the river and carries a very heavy traffic load, in addition to its weight and earthquake loads. It was determined because of the analyses that, in the strained regions of the bridge, stones should be joined to each other with iron clamps to eliminate tensile stresses. Furthermore, the sections should be enlarged and wooden elements should be used on the foundations where the abutments of the arches are located, as in the historical bridge construction technique [34, 39] Moreover, this study demonstrated that not only linear analyses but also nonlinear analyses of these types of historical works should be performed, as they can yield very different results. Considering the bridge geometry, it is expected that stress and deformation values will increase on the arch, which has more flatness than other regions of the bridge. It should not be ignored that this method will create a weak zone in the load-carrying system of the bridge. One study state [30] that arches with high flatness cannot be found in the original form of this type of bridge. In other words, the builders and architects who built these ancient structures were aware of this unfavorable situation. Considering all the analysis results, the most important points were the integration of stone elements constituting the bridge and the stability of the bridge abutments. This study's results are expected to guide future restoration and renovation efforts.

REFERENCES

- [1] N. Ademovic. (2016). Structural repair of Careva Cuprija Bridge in Sarajevo. *Gradevinar*, 68(12), 995–1008.
- [2] N. Ademovic, & A. Kurtovic, (2018). Seismic performance and retrofit of a historic monument arch bridge. Paper presented at the 16th European Conference on Earthquake Engineering 16ECEE, Thessaloniki Greece.
- [3] A. Akhaveissy, A. Permoon, & R. Raeisi. (2021). Numerical modeling of masonry wall under underground waves. *Scientia Iranica*. 28(6), 2987–3007, doi: 10.24200/sci.2021.53605.3327
- [4] A. H. Akhaveissy. (2011). Lateral strength force of URM structures based on a constitutive model for interface element. *Latin American Journal of Solids and Structures*, 8(4), 445–461.
- [5] A. Alkan, O. Baykan, A. Atalay, N. Baykan, & Ü. S. Öziş. (2011, 16-18 Eylül 2011). Su Yapısı Olarak Anadolu'daki Taş Köprüler (Masonry Bridges in Anatolia as a Water Structure). Paper presented at the II. Su Yapıları Sempozyumu, Diyarbakır, Türkiye.
- [6] A. C. Altunisik, B. Kanbur, & A. F. Genc. (2015). The effect of arch geometry on the structural behavior of masonry bridges. *Smart Structures and Systems*, 16(6), 1069-1089, doi: 10.12989/sss.2015.16.6.1069
- [7] ANSYS. (2015). Inc. Products Release 17.0, Finite element analysis program. USA.
- [8] S. Ataei, M. Jahangiri Alikamar, & V. Kazemiashtiani. (2016). Evaluation of axle load increasing on a monumental masonry arch bridge based on field load testing. *Construction and Building Materials*, 116, 413–421, doi: 10.1016/j.conbuildmat.2016.04.126
- [9] T. T. Bui, A. Limam, & Q. B. Bui. (2014). Characterisation of vibration and damage in masonry structures: Experimental and numerical analysis. *Eur. J. Environ. Civ. Eng.*, 18(10), 1118–1129.
- [10] F. Cakir, & B. Seker. (2015). Structural Performance of Renovated Masonry Low Bridge in Amasya, Turkey. *Earthquakes and Structures*, 8(6), 1387–1406, doi: 10.12989/eas.2015.8.6.1387
- [11] Z. Celep. (2017). Deprem Mühendisliğine Giriş ve Deprem Dayanıklı Yapı Tasarımı (Introduction to Earthquake Engineering and Earthquake Resistant Structure Design). Istanbul:Beta Yayınları.
- [12] C. Çulpan. (2002). Türk Taş Köprüleri, Ortaçağdan Osmanlı Devri Sonuna Kadar (Turkish Masonry Bridges, From the Middle Ages to the End of the Ottoman Period). Ankara:Türk Tarih Kurumu Basımevi.
- [13] K. D. Dalgıç, (2010). Düşük Elastisite Modüllü Cam Lifli Polimerle Sargılanmış Düşük Dayanımlı Betonun Eksenel Yükler Altında Davranışı ve Sonlu Eleman Metodu ile Analizi (Behavior of Low Strength Concrete Wrapped with Low Modulus Glass Fiber Polymer Under Axial Loads and Analysis by Finite Element Method). Master Thesis (in Istanbul), İTÜ, Turkey.
- [14] T. Karabörk, T. Çelik, & A. Ural, (2016). Finite element analyses of historical Bıçakçı arch bridge, Turkey. Paper presented at the 8th International Conference on Arch Bridges ARCH2016, Wrocław Poland.
- [15] M. Karaton, H. S. Aksoy, E. Sayın, & Y. Calayır. (2017). Nonlinear seismic performance of a 12th century historical masonry bridge under different earthquake levels. *Engineering Failure Analysis*, 79, 408–421, doi: 10.1016/j.engfailanal.2017.05.017
- [16] A. Kindij, A. M. Ivankovic, & M. Vasilj, (2013). Assessment of masonry arch bridge with concrete deck. Paper presented at the 7th International Conference on Arch Bridges, ARCH'13, Trogir-Split, Croatia.
- [17] G. Lacidogna, & F. Accornero. (2018). Elastic, plastic, fracture analysis of masonry arches: A multi-span bridge case study. *Curved and Layered Structures*, 5(1), 1–9, doi: 10.1515/cls-2018-0001
- [18] B. M., G. L., & V. A. (2015). Time-History Seismic Analysis of Masonry Buildings: A Comparison between Two Non-Linear Modelling Approaches. *Buildings*, 5(2), 597–621, doi: 10.3390/buildings5020597
- [19] D. Malomo, R. Pinho, & A. Penna. (2018). Using the applied element method for modelling calcium silicate brick masonry subjected to in-plane cyclic loading. *Earthquake Engineering and Structural Dynamics*, 47, 1610–1630, doi: 10.1002/eqe.3032
- [20] D. V. Oliveira, & P. B. Lourenço, (2004). Repair of Masonry Arch Bridges. Paper presented at the Arch Bridges ARCH'04, Barselona.
- [21] D. V. Oliveira, & P. B. Lourenço, (2006). Repair of a historical stone masonry arch bridge. Paper presented at the The Third International Conference on Bridge Maintenance.
- [22] D. V. Oliveira, P. B. Lourenço, & C. Lemos. (2010). Geometric issues and ultimate load capacity of masonry arch bridges from the northwest Iberian Peninsula. *Engineering Structures*, 32(12), 3955–3965, doi: 10.1016/j.engstruct.2010.09.006
- [23] A. Özmen, & E. Sayın. (2018). Seismic assessment of a historical masonry arch bridge. *Journal of Structural Engineering & Applied Mechanics*, 1(2), 95–104, doi: 10.31462/jseam.2018.01095104

- [24] A. Özmen, & E. Sayın, (2018). Seismic Behaviour of Mavilik Masonry Arch Bridge. Paper presented at the International Engineering and Natural Sciences Conference INESEG, Diyarbakır, Turkey.
- [25] A. Özmen, E. Sayın, (2018). & Linear Dynamic Analysis of a Masonry Arch Bridge. Paper presented at the International Conference on Innovative Engineering Applications CIEA'2018, Sivas, Turkey.
- [26] A. Paeglitis, A. Paeglitis, I. Vitiņa, & S. Igaune. (2013). Study and Renovation of Historical Masonry Arch Bridge. *The Baltic Journal of Road and Bridge Engineering*, 8(1), 32–39, doi: 10.3846/bjrbe.2013.05
- [27] B. Riveiro, J. Armesto, P. Arias, & F. Rial. (2008). Multidisciplinary approach to historical arch bridges documentation. *Int Arch Photogramm Remote Sens Spat Inf Sci*, 247–252.
- [28] T. S., & M. G. (2017). Historic City Centers After Destructive Seismic Events, The Case of Finale Emilia During the 2012 Emilia-Romagna Earthquake: Advanced Numerical Modelling on Four Case Studies. *Open Civil Engineering*, 11(1), 1059–1078.
- [29] E. Sayın, & M. Y. Karaton, (2011). Nonlinear seismic analysis of historical Uzunok bridge. Paper presented at the 7. Uusal Deprem Mühendisliği Konferansı, İstanbul, Turkey.
- [30] M. E. Stavroulaki, (2008). Parametric Finite Element Analysis of Masonry Structures Using Different Constitutive Models. Paper presented at the In 6th GRACM International Congress on Computational Mechanics, Thessaloniki, Greece.
- [31] B. Ş. Şeker, & M. Gökçe. (2021). Tarihi Hundi Hatun (Kunç) Köprüsünün Artan Trafik Yükü Altında Davranışının İncelenmesi (Investigation of Historical Hundi Hatun (Kunç) Bridge's Behavior Under Increasing Traffic Load). *International Journal of Engineering Research and Development*, 13(2), 496–507, doi: doi: 10.29137/umagd.823912
- [32] Ş. Şeker. (2020). Author Archive.
- [33] M. E. Tomazevic. (1999). Earthquake-Resistant Design of Masonry Buildings. London:Imperial College Press.
- [34] G. Uruk, (1994). Amasya'nın Türk Devri Şehir Dokusu ve Yapılarının Analiz ve Değerlendirilmesi (Analysis and Evaluation of Amasya's Turkish Period Urban Texture and Structures). PhD Thesis (in Ankara), Gazi University, Turkey.
- [35] URL-1. Anonymous. (2002). Retrieved 06.10.2020, from https://2.bp.blogspot.com/-3nL2NZ9-BCs/XFR74UqyhKI/AAAAAAAAAuys/5s_pHnBf8dMDj9lcpDFtsebkl_GgcV4mQCLcBGAs/s1600/amasya_merkez.jpg
- [36] URL-2. Johnson and Stern. (2010). from <https://africa-arabia-plate.weebly.com/arabian-plate.html>
- [37] URL-3. Disaster and Emergency Management Presidency Department of Earthquake. (2020) Retrieved 06.10.2020, from <http://kyhdata.deprem.gov.tr>
- [38] URL-4. T. R. General Directorate of Foundations. (2017). Tarihi Yapılar İçin Deprem Risklerinin Yönetimi Kılavuzu (Earthquake Risk Management Guide for Historic Buildings). Retrieved 06.10.2020, from https://cdn.vgm.gov.tr/organizasyon/organizasyon12_030619/kilavuz.pdf
- [39] URL-5. Anonymous. (2017). Retrieved 06.10.2020, from <https://www.youtube.com/watch?v=FE5TnbedRuo>
- [40] P. Zampieri, M. A. Zanini, F. Faleschini, L. Hofer, & C. Pellegrino. (2017). Failure analysis of masonry arch bridges subject to local pier scour. *Engineering Failure Analysis*, 79, 371–384. doi: 10.1016/j.engfailanal.2017.05.028